

82-9-318

DEUTSCHES ELEKTRONEN-SYNCHROTRON **DESY**

DESY 82-055
August 1982

OBSERVATION OF TOPOLOGICALLY ISOLATED ENERGETIC ELECTRONS

IN e^+e^- INTERACTIONS

by

CELLO Collaboration

NOTKESTRASSE 85 · 2 HAMBURG 52

DESY behält sich alle Rechte für den Fall der Schutzrechtserteilung und für die wirtschaftliche Verwertung der in diesem Bericht enthaltenen Informationen vor.

DESY reserves all rights for commercial use of information included in this report, especially in case of filing application for or grant of patents.

**To be sure that your preprints are promptly included in the
HIGH ENERGY PHYSICS INDEX,
send them to the following address (if possible by air mail) :**

**DESY
Bibliothek
Notkestrasse 85
2 Hamburg 52
Germany**

OBSERVATION OF TOPOLOGICALLY ISOLATED ENERGETIC ELECTRONS

IN e^+e^- INTERACTIONS

CELLO COLLABORATION

H.-J. BEHREND, C. CHEN¹, H. FENNER, M.J. SCHACHTER, V. SCHRODER, H.SINDT,
Deutsches Elektronen Synchrotron, Hamburg, Germany.

G. D'ACOSTINI, W.D. APEL, S. BANERJEE, J. BODENKAMP, D. CHROBACZEK,
J. ENGLER, G. FLÜGGE, D.C. FRIES, W. FUES, K. GAMERDINGER, G. HOPP,
H. KÜSTER, H. MÜLLER, H. RANDOLL, G. SCHMIDT, H. SCHNEIDER,
Kernforschungszentrum Karlsruhe and Universität Karlsruhe, Germany.

W. DE BOER, G. BUSCHORN, G. GRINDHAMMER, P. GROSSE-WIFSMANN,
B. GUNDERSON, C. KIESLING, R.KOTTHAUS, U. KRUSE², H. LIERL, D. LÜERS,
H. OBERLACK, P. SCHACHT,
Max Planck Institut für Physik und Astrophysik, München, GERMANY.

P. COLAS, A. CORDIER, M. DAVIER, D. FOURNIER, J.F. GRIVAZ,
J. HAÏSSINSKI, V. JOURNÉ, A. KLARSFELD, F. LAPLANCHE, P. LE DIBERDER,
U. MAILLIK, J.J. VEILLET,
Laboratoire de l'Accélérateur Linéaire, ORSAY, France.

J.H. FIELD, R. GEORGE, M. GOLDBERG, E. GROSSETÊTE, O. HAMON, F. KAPUSTA,
F. KOVACS, G. LONDON, L. POGGIOLI, M. RIVOAL.

Laboratoire de Physique Nucléaire et Hautes Energies, Paris, France.

R. ALEKSAN, J. BOUCHEZ, G. CARNESECCHI, C. COZZIKA, Y. DUCROS,
A. GAIDOT, S. JADACH³, Y. LAVAGNE, J. PAMELA, J.P. PANSART, F. PIERRE,
DFHPE, Centre d'Etudes Nucléaires, Saclay, France.

1 - Visitor from the Institute of High Energy Physics, Chinese Academy of Science,
Peking, People's Republic of China

2 - Visitor from University of Illinois, Urbana, USA.

3 - Visitor from the University of Cracow, Poland.

ABSTRACT

In e^+e^- interactions at 34 GeV center of mass energy, using an integrated luminosity of 7.4 pb^{-1} , 18 events are observed where an electron (positron) appears with an energy above 4 GeV, at large angle with respect to the beam direction, and well separated from other emerging charged and neutral particles. The characteristics of these events are found to be in agreement with the event characteristics expected from deep inelastic electron photon scattering and inelastic Compton scattering, together with at most a small contribution from multihadron annihilation.

INTRODUCTION

During the scanning of multiparticle events collected by the CELLO detector at PETRA, we have observed several events where an electron (e^+ or e^-) was produced in association with a hadronic system, in which most of the particles go into the hemisphere opposite to the electron. The strong forward peaking observed in the electron polar angular distribution suggests that these events were produced by a non-annihilation mechanism. In order to measure this effect quantitatively, we have made a systematic search. After a review of the experiment, we describe this search, and compare the characteristics of the observed events with expectations from deep inelastic electron photon scattering, inelastic Compton scattering and e^+e^- annihilation into hadrons.

EXPERIMENT

The CELLO detector has been previously described [1]. Let us mention the main features relevant for this analysis: Constraining the tracks to the beam position, the central detector measures the momentum of charged particles with $dP/P = P \text{ (GeV/c)} \times 0.02$ for track angles, θ , with respect to the beam direction between 30 and 150 degrees.

Electromagnetic calorimetry is provided over the same solid angle by a lead-liquid argon counter, 20 radiation lengths thick. The longitudinal development of the showers is analysed in 6 layers. The energy resolution, σ_E/E , determined from photons and electrons in Bhabha events, can be described by $13\%/\sqrt{E}$.

Various triggers, utilizing charged particles, neutral particles, and combinations of both, give an efficiency of >99% on multiparticle events.

The data reported here were collected at 17 GeV beam energy during the first half of 1981. The integrated luminosity is 7.4 pb^{-1} .

ELECTRON SEARCH

A computer search was performed in order to be able to measure quantitatively and to compare with the Monte Carlo simulations of theoretical models.

Selected events were required to have at least four charged tracks and an isolated track with a momentum greater than 4 GeV/c.

An isolated track was defined by $P_{\parallel}^{\pm} < 1 \text{ GeV}/c$ and $P_{\parallel}^0 < 2 \text{ GeV}/c$, where P_{\parallel}^{\pm} (P_{\parallel}^0) denotes the sum of the momenta of the charged (neutral) particles in the same hemisphere as the isolated track projected onto the direction of the isolated track.

These cuts were chosen to remove most of the events coming from multihadronic production through one photon exchange. The neutral particle cut is softer because the calorimetric measurement is less precise than the central detector measurement and to avoid rejecting electrons accompanied by a soft bremsstrahlung photon.

Finally, we demanded that the effective mass of the charged particles recoiling against the isolated track be larger than $2 (\text{GeV}/c)^2$. This last cut removed contamination from τ pair production and radiative Bhabha events.

Events surviving the above selection were then visually scanned by physicists to reject residual background.

After the scan, the electron was identified according to two criteria: The calorimetric energy E must agree with the momentum P measured in the central detector and the longitudinal development of the shower must be consistent with the expected development of an electromagnetic shower. According to simulation of shower development, measurement on test shower counters and observation in Bhabha events, the fraction of the energy deposited in layers 2 and 3 of the calorimeters, F_{23} , is sensitive to the difference between electromagnetic shower development and hadronic shower development. Figure 1 shows a scatter plot of F_{23} vs. E/P . A significant signal appears for E/P around 1 and larger F_{23} , as expected for electrons showering in the detector, against a background due to isolated hadrons. Electrons were defined as those tracks for which

$$0.5 < E/P < 2.0, F_{23} > 20\% \text{ and } E_6 < 500 \text{ MeV},$$

where E_6 is the energy measured in the 6th layer.

After this selection, 18 events remain, corresponding to a detected cross section of 2.4 ± 0.6 (stat.) ± 0.3 (syst.) pb.

The systematic error takes into account uncertainties in luminosity, event selection and shower reconstruction efficiency. The contamination from annihilation events is not included here and will be treated in the next chapter.

INTERPRETATION

Several mechanisms can be invoked to interpret these data.

The first one which has been considered is the reaction:

$$e^+ e^- \rightarrow e^+ e^- + X \quad (1)$$

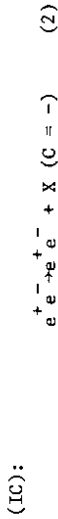
where X is a hadronic system. When one of the emerging electrons is at large transverse momentum, this process is called deep inelastic electron-photon scattering (DIS), the target photon being a quasi-real one emitted by the electron scattered at small angle. The squared four momentum transfer from the large transverse momentum electron to the target photon is denoted by Q^2 in the following. The corresponding Feynman graph is shown in Fig. 2a. The X system has positive charge

conjugation quantum number. Measurements of this process for values of the electron scattering angle, θ , between 100 and 400 mrad have been reported [2].

The contribution of reaction (1) has been computed by generating events using the structure function given in Ref. [3], which takes into account contributions from vector dominance (Fig. 2b), the quark parton model (Fig. 2c), and QCD corrections to the quark-parton model (Fig. 2d). The value of the QCD scale parameter, A , used in the structure function was 0.1 GeV. Only leading order terms for the structure function were considered.

The hadronic part X has been generated as a quark-antiquark system (u,d,s,c), including gluon emission, fragmenting into hadrons with a limited transverse momentum distribution with respect to the directions of the parent partons. The events so generated were propagated through the detector and analysed with the same cuts as the real data. The predicted number of events is 9.3.

A second possible process is inelastic Compton scattering



This can be considered as a radiative Bhabha process, where a real photon is replaced by a massive one, which converts to a hadronic system X (Fig. 2e). A simulation procedure, similar to the one used for reaction (1), has been applied to reaction (2) and predicts 4.6 events [3].

Finally we have considered annihilation into hadrons:



which can contribute to the observed events through several mechanisms: hadron misidentification, very asymmetric photon conversion, Dalitz decay, or prompt electron emission via charm or beauty decay. The sum of all these mechanisms has been estimated by means of the detector simulation, using two different models for particle generation [4, 5]. Radiative corrections, c and b quark production and decay, and gluon emission are taken into account. These models have been used with para-

eters which reproduce the general characteristics of multihadronic events [6]. The expected number of events is 4.5 ± 4.5 , the error being a systematic one which reflects uncertainty in the modelling.

A summary of a comparison between the experimental data and the predictions for reactions (1) to (3) is presented in Table 1, where averages of several significant quantities as measured in the data or as expected from the Monte Carlo calculations are reported. Corresponding distributions for the data are shown in Figs. 3 and 4a to 4f, together with the simulation of the sum of the non-annihilation processes (reactions (1) and (2)).

From the angular distribution (Fig. 3) and the longitudinal momentum (P_z) distribution (Fig. 4f) - which are expected to be symmetric for reaction (3) - we see that the bulk of the observed events comes from a non-annihilation process. This confirms the dominance of reactions (1) and (2) more strongly and independently of the cross section comparison. In particular, the asymmetry of the P_z distribution expresses the fact that some energetic particle(s) is (are) going at small angle along the beam line, opposite to the incoming electron of the same sign as the isolated electron (The corresponding transverse momentum distribution has an average of 1.9 GeV/c, consistent with the experimental resolution).

However, quantitative agreement between the Monte Carlo calculation for reactions (1) and (2) and the data is not good, especially for the angular distribution (Fig. 3) and the mass of the recoil system, as measured from the charged particles (Fig. 4b) or from charged and neutral particles (Fig. 4e). The discrepancies point towards some contribution from the annihilation process.

Relative enhancement of reaction (1) can be achieved by selecting events for which $\cos \theta > 0$ and $P_z < 0$. We observed 11 events at an average Q^2 of 118 (GeV/c)² to be compared to expected numbers of 8.1, 2.5 and 1.1 ± 1.1 for reactions (1), (2), and (3) respectively. In particular, by subtracting the expected contributions of reactions (2) and (3) from the real data, we get 7.4 ± 3.9 events to be compared to the prediction of 8.1.

This first investigation of deep inelastic electron photon scattering at large Q^2 is consistent with the $\log(Q^2)$ dependence of the photon structure function predicted by the theory [3]. However, the quark parton picture for the structure function cannot be excluded on the basis of the present statistics.

More detailed comparison between models and data would require more data.

We have not considered the production of new particles, such as pair-production of a sequential heavy lepton, technipion etc. ... for which there is no evidence so far. We decided to limit our analysis to reactions which are known to exist at this energy. It is clear that the discovery of such new particles would alter the quantitative analysis presented here.

CONCLUSION

In e^+e^- multiparticle production at 34 GeV center of mass energy, we have observed 18 events with an energetic isolated electron. The bulk of these events can be interpreted as coming from two non-annihilation processes: deep inelastic electron-photon scattering at Q^2 of the order of 100 $(\text{GeV}/c)^2$ and inelastic Compton scattering. More data should allow a measurement of the photon structure function in the very high Q^2 region.

REFERENCES

[1] CELLO Coll., H.J. Behrend et al., Phys. Scripta 23 (1981) 610
 [2] PLUTO Coll., Ch. Berger et al., Phys. Letters 107B (1981) 19;
 JADE Coll., quoted by J.H. Field in the proceedings of the XVIIth Rencontre de Moriond (1982), Ed. Frontières;
 CELLO Coll., J. Häüssinski, LAL 82/11 (XVIIth Rencontre de Moriond, 1982)
 [3] C. Peterson et al., Nuclear Phys. B174 (1980) 424
 [4] B. Anderson et al., Z. Phys., Particles and Fields C6 (1980) 235;
 T. Sjostrand, LU-TP-80-3 (1980);
 B. Anderson et al., LU-TP-81-3 (1981)
 [5] P. Hoyer et al., Nuclear Phys. B161 (1979) 349
 [6] CELLO Coll., H.J. Behrend et al., Phys. Letters 110B (1982) 329
 and to be published

FIGURE CAPTIONS

Fig. 1: Scatter plot of E/P and P_{23} (see text) for selected isolated charged tracks

Fig. 2: a) Feynman diagram for reaction (1)
 b) Diagram for vector dominance model
 c) Diagram for quark-parton model
 d) One diagram of QCD correction to the quark-parton model
 e) Feynman diagrams for reaction (2)

Fig. 3: $\cos \theta$ distribution, where θ is the angle between the outgoing detected electron and the incoming electron of the same sign

Fig. 4: Distributions

- a) Momentum of isolated track
- b) Effective mass of recoil system (charged particles only)
- c) Charged multiplicity
- d) $Q^2 = -$ transverse momentum squared between detected electron and incident electron of the same sign
- e) Effective mass of recoil system (all detected particles)
- f) P_z = projection on the beam direction of the momentum vector sum of all detected particles. The beam direction is oriented along the incident electron whose sign is opposite to the isolated one

	DATA	Deep Inelastic Scattering DIS	Inelastic Compton Scattering ICS	Multihadrons	DIS + ICS
Momentum (GeV/c) of isolated electron	9.6 ± 0.8	10.2	8.5	7.7	9.6
Recoil system mass (GeV/c ²) (charged only)	5.2 ± 0.5	4.3	3.4	5.5	4.0
Charged multiplicity	8.3 ± 0.7	7.7	7.3	9.1	7.6
$\cos \theta$ θ is the angle between the outgoing detected electron and the incoming electron of the same sign.	0.37 ± 0.10	0.70	0.13	0.	0.51
Q^2 (GeV ²) Transverse momentum squared between detected electron and incident electron of the same sign.	160. ± 20.	95.1	161.	160.	114.
Recoil system mass (GeV/c ²) (all detected particles)	8.6 ± 0.7	7.1	5.3	9.9	6.5
P_z (GeV/c) Projection on the beam direction of the momentum vector sum of all detected particles. The beam direction is oriented along the incident electron whose sign is opposite to the isolated one.	-4.7 ± 1.0	-5.7	-5.5	0.	-5.6
Events	18	9.3	4.6	4.5 ± 4.5	13.9

TABLE 1 - Averages and event numbers for data and simulations

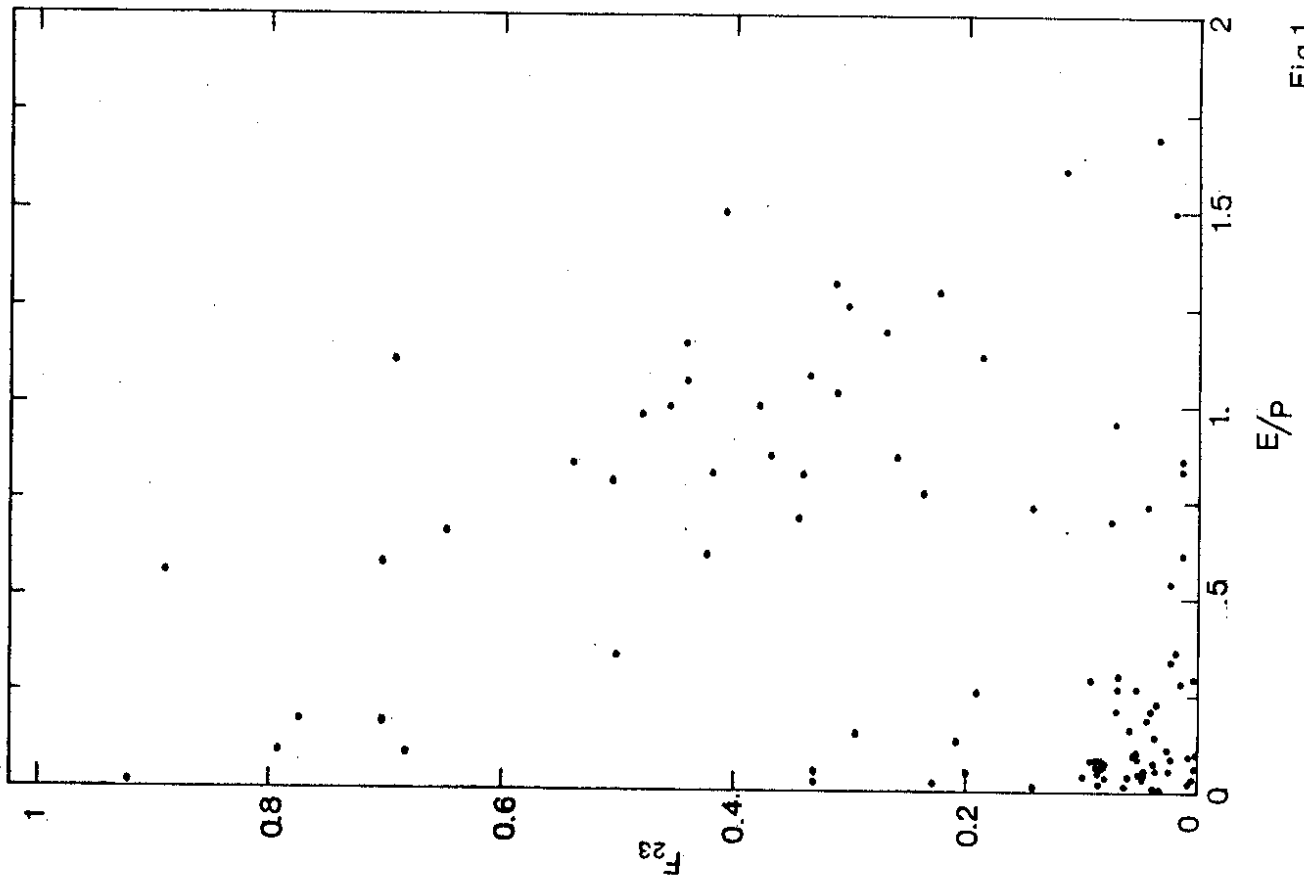
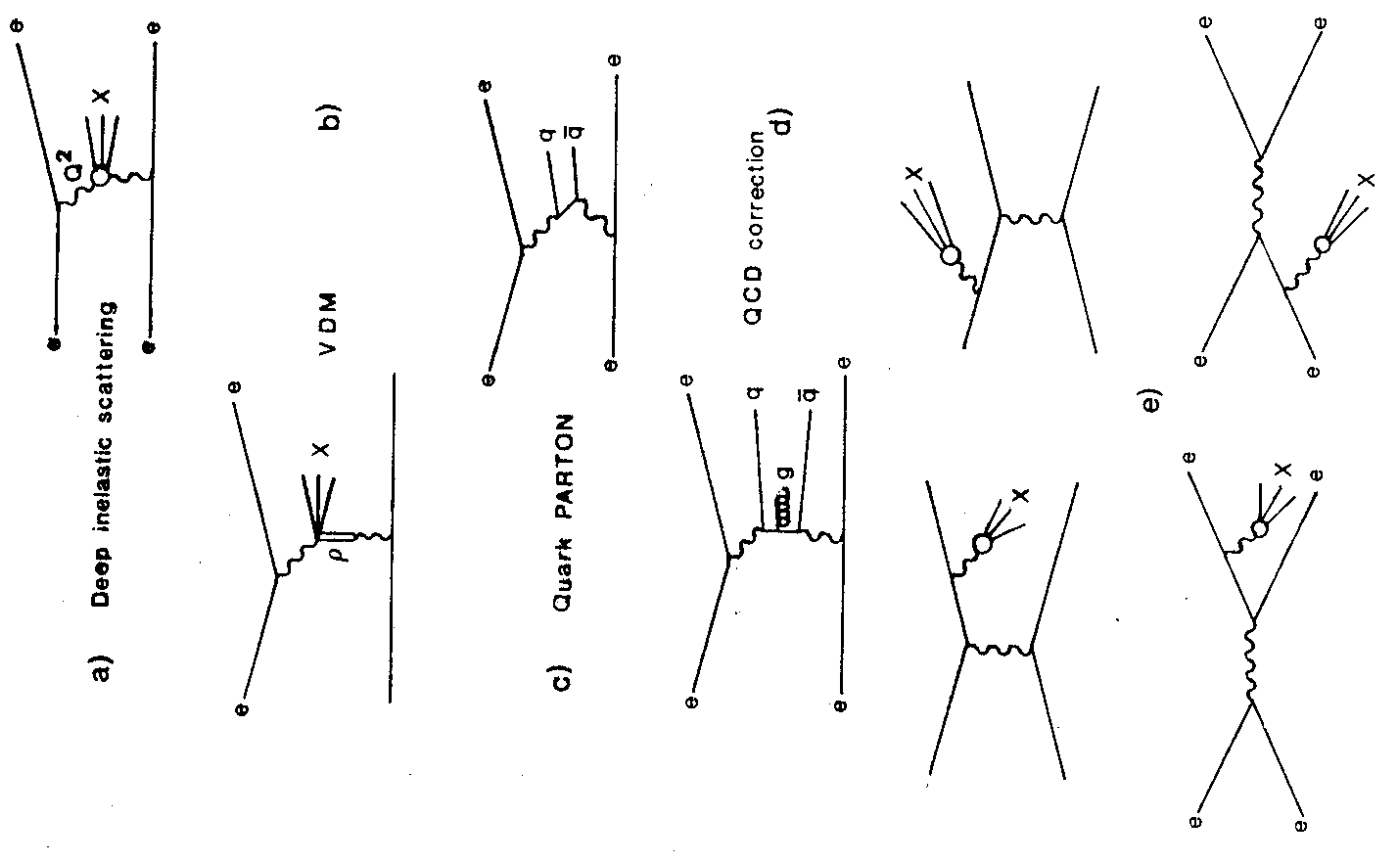


Fig.1



Inelastic Compton scattering

Fig.2

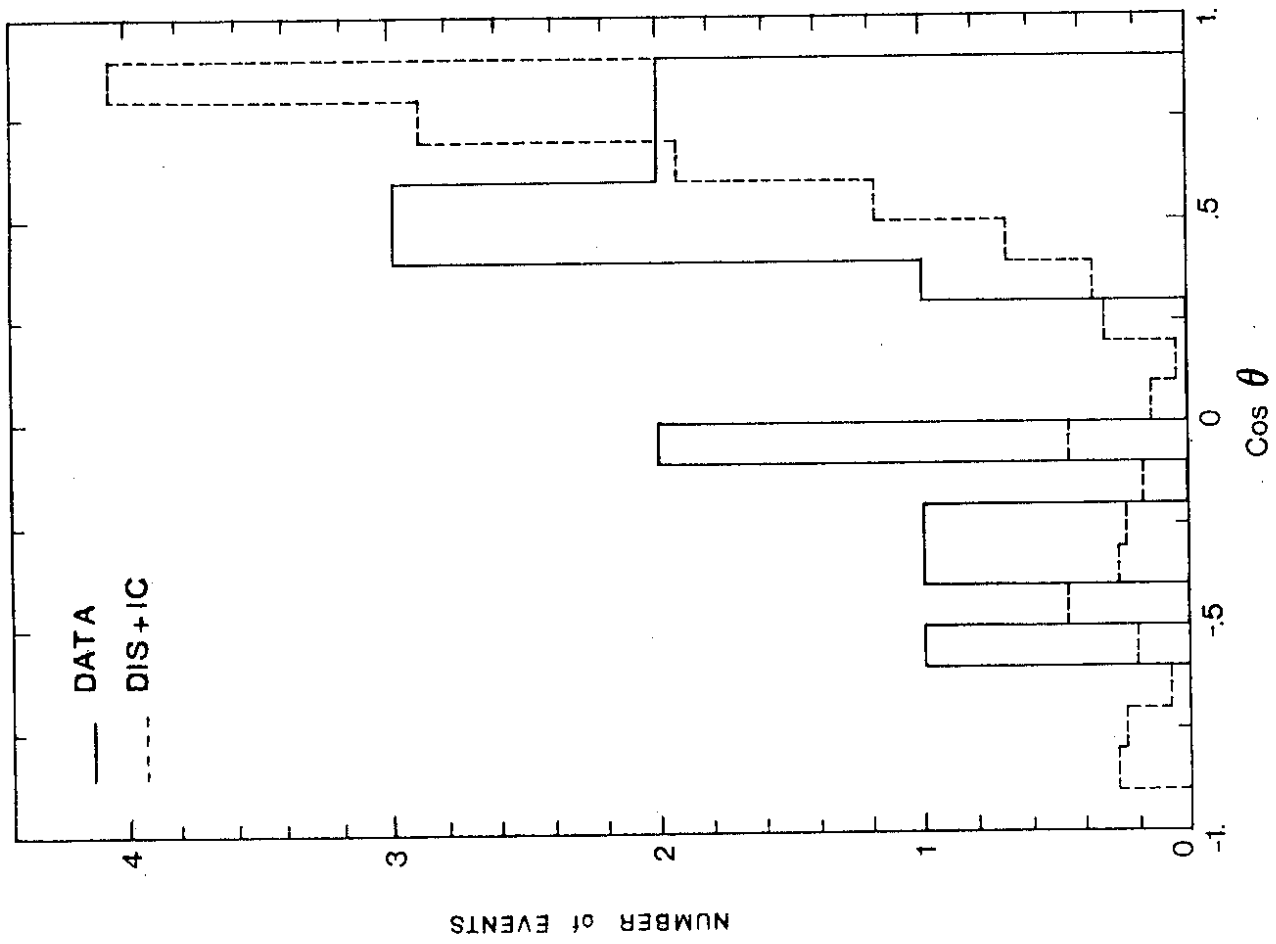


Fig.3

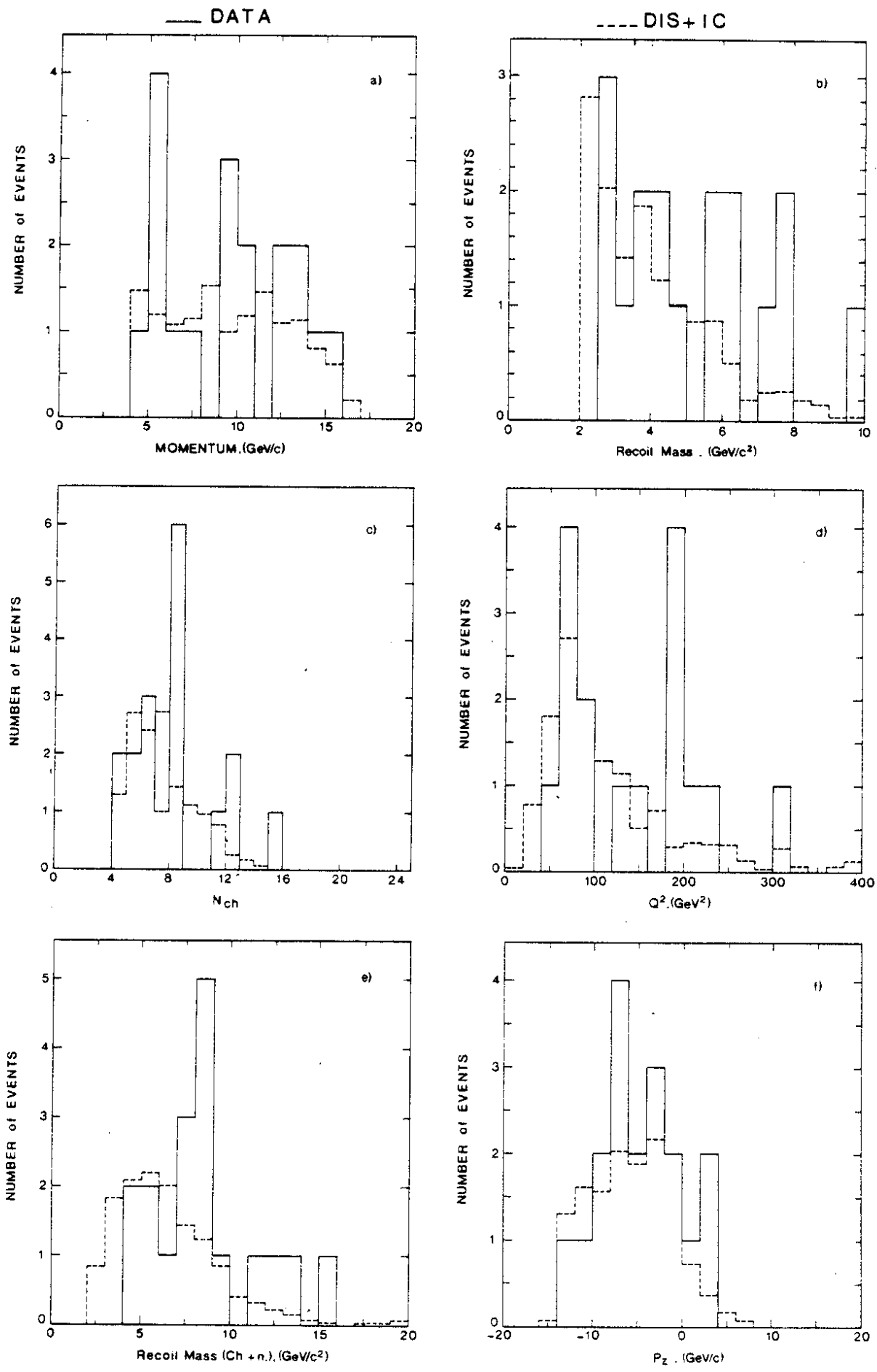


Fig. 4